**Abdelkader ABDELDJEBBAR[1]*, Azzedine HAMID[1], Yacine GUETTAF[2], Rabia MELATI[1]**

[1] Laboratory of Applied Power Electronics (LEPA), University of Sciences and Technology Mohamed Boudiaf of Oran (USTO-MB), ALGERIA.
[2] University Center Nour Bachir of El Bayadh, ALGERIA.

doi:10.15199/48.2018.08.22

# Design of Micro-Transformer in Monolithic Technology for High Frequencies Fly-back Type Converters

***Abstract:*** *The work presented in this article concerns the design of micro-transformer in Monolithic Technology for High Frequencies comprised of planar type coil and a magnetic circuit made of several layers of materials. This micro-transformer will be integrated into a micro-converter of type Fly-back. The Mohan method for determining the geometric parameters and the use of S-parameters for the calculation of technological parameters was chosen. The electrical model in π presented, perfectly summarizes the various parasitic effects generated by stacking layers of different materials constituting the micro-transformer. The study of electromagnetic effects allowed us to show the role of ferrite, which is used to confine the magnetic field lines and minimize disruption of the neighbor ship. To validate dimensioning of the geometrical and technological parameters, we have simulated with the help of the software PSIM 6.0, the equivalent electrical circuit of the converter containing the electrical circuit of the dimensioned planar micro-transformer.*

***Streszczenie.*** *W artykule zaprezentowano projekt planarny wysokoczęstotliwościowy mikrotransformator w technologii monolitycznej. Do projektowania geometrii wykorzystano metodę Mohana a do projektu technologii wykorzystano metodę S-parameters. Właściwości zaprojektowanego transformatora analizowano metodami symulacyjnymi.* ***Projekt wysokoczęstotliwościowego mikrotransformatora w zastosowaniu do przekształtników***

**Keywords**: Fly-back Converter, Planar Micro-Transformer, S-Parameters, inductive elements, passive.
Słowa kluczowe: mikrotransformator planarny, przekształtnik flyback

## Introduction

The passive components occupy 80% of the surface of a low-power converter. They have several roles, such as temporary storage of electrical energy, filtering, electrical isolation, energy transfer as well as the impedance matching. Today, only the integration of passive components is achievable, especially inductive components. The barrier of integrating active components remains the most persistent obstacle that slows the rush to miniaturization [1] [2]. At the heart of isolated converters, there exists an essential element, the transformer. By reducing the dimensions, limited conventional coils since they are wound with copper wire which prevent reducing the size. To overcome this problem, the planar components were introduced. The micro-transformers are formed by a thin magnetic circuit, usually made of ferrite, and on which conductive coils are inserted. The aim is to integrate the transformer in a micro-converter of flyback type for the low voltages, the low powers and the high frequencies. The conception of a transformer goes through several phases: analysis of specifications, calculation and dimensioning of transformer parameters and validation by numerical simulation. In this work, the micro-transformer is presented under a form completely different to geometric form of a classical transformer. This geometry is square spiral, it adapts to the integration technology [3] [4].

## Dimensioning of The Micro Transformer

### *Presentation of micro transformer*

The micro converter fly-back presented in Figure 1, is the starting point for the design of passive components and especially, the micro transformer. The choice of this converter is because it is composed of a transformer and few passive components. It operates in discontinuous conduction when the current demanded by the load is low, and in continuous conduction for higher currents. This functional integration is illustrated in Figure 2. To produce such a device, we start with conventional transformer windings. To implement this function, it is necessary to have a magnetic core around which are placed the primary and secondary windings. This transformer, due to the magnetic coupling, naturally induces the effects of leakage mainly related to the choice of placement of windings.

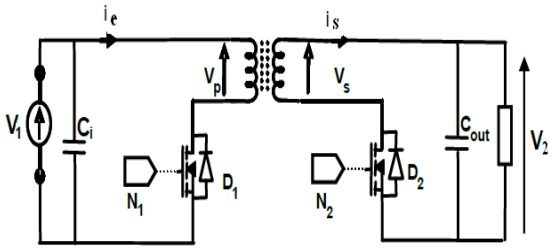


Fig 1: Schematic diagram of fly back converter [5]

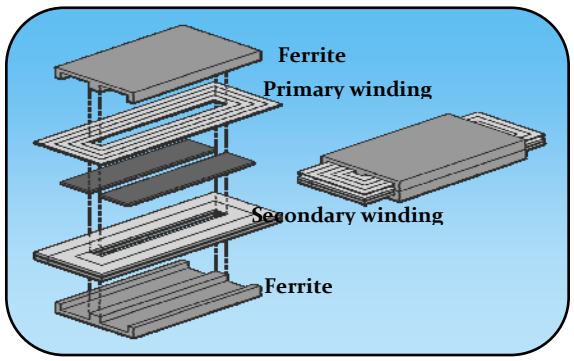


Fig.2: View of an integrated micro-transformer [6]

### *The specifications of the micro-converter*

We selected the following set of specifications:
Input voltage $V_{in}$ = 10v
Output voltage $V_{out}$ = 4v
Current output means Is = 1.5A
Average power Ps = 6W
Operating frequency f = 40MHz

### *Characteristics of used materials*

The table below shows the characteristics of materials constituting the coil layers.

Table 1: characteristics of used materials

| Materiel | Copper | NiFe | $SiO_2$ |
|---|---|---|---|
| Conductivityσ (S/m) | $5{,}99.10^{7}$ | $2{,}2.10^{4}$ | 0 |
| Resistivity ρ (Ω.m) | $1{,}7.10^{-8}$ | $20.10^{-8}$ | $>10^{5}$ |
| Relative Permittivity $\varepsilon_r$ | 1 | 10 | 3,9 |
| Relative permeability $\mu_r$ | 1 | 800 | 1 |

Fig. 3 shows the different geometric and electrical parameters that constitute the micro transformer figure 3 [7]. A core with a square form for the windings has been chosen due to the limitation of surface and volume.

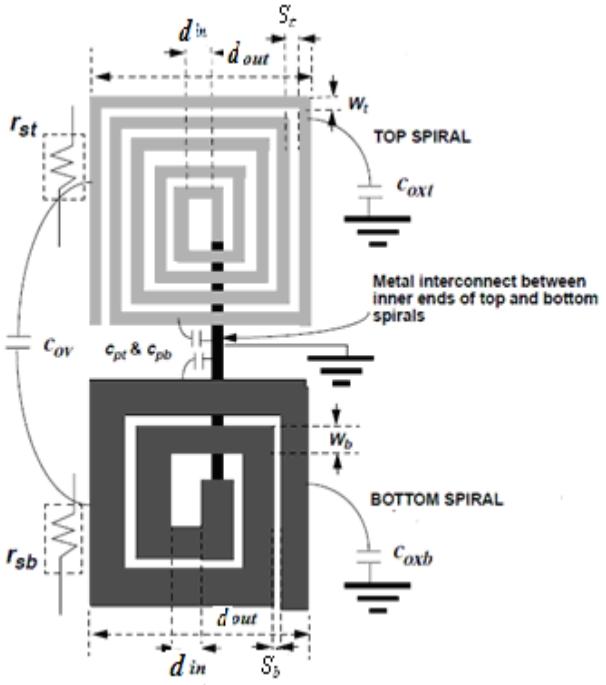


Fig.3 : The different parameters characterizing the micro-transformer [8]

***Dimensioning of the magnetic circuit***

From the specifications, we define the characteristics of micro-converter that is the starting point for the design of micro-transformer. It consists of two inductors placed on a magnetic material and separated by a dielectric which also provides magnetic coupling. The values of the frequency f and the input voltage $V_e$ allow us to calculate the value of the primary and secondary inductances $L_t$ and $L_b$ of our transformer [8][9].

(1) $$L_t = \frac{V_e^2 \alpha^2}{2 f P_s}$$

(2) $$L_b = m^2 L_t$$

(3) $$m = \frac{1 - V_s \alpha}{\alpha V_e}$$

m: turn ratio=0.4; $L_t$ = 52nH; $L_b$ = 8.3nH

*Calculation of the energy stored in the magnetic core*

The dimensioning of the magnetic core depends on the volume required to store energy which is calculated from the volumetric energy density [10] given by equation 4.

(4) $$W = \frac{1}{2} L_t i_e^2 = \frac{1}{2} L_b i_s^2 = 937.10^{-9}\, j$$

*Calculation of the volume density of energy*

To determine the volume V of permalloy (NiFe) necessary for this storage, we need to know the volume density of energy of this material. This volume V is given by relationship 5 [11]:

(5) $$V = \frac{W}{W_{max}}$$

With

(6) $$W_{\max} = \frac{B_{\max}^2}{2 \mu_0 \mu_r}.$$

With a relative permeability $\mu_r = 800$ and saturation induction $B_{max} = 0.6\ T$ of permalloy, we obtain: $W_{max} = 179\ jm^{-3}$, and $V = 0.052 mm^3$

So, 0.052 mm$^3$ of Nife is needed to store 0,937 µJ.

*Core dimensions*

The volume of the ferromagnetic core being evaluated $\left(V = 0.052\ mm^3\right)$, We consider the core as a block having a thickness $e_{Nife}$ and a section $A = \left(d_{out}\right)^2$, S is the section on which we will put the spiral coil. To define the dimensions of the core, we opted for $d_{out} = 1800 \mu m$ and we calculate the section $A$ and the thickness core $e_{Nife}$ by using equation 7 $A = 324.10^4\ \mu m^2$

(7) $$e_{Nife} = \frac{V}{A} = 16.15 \mu m$$

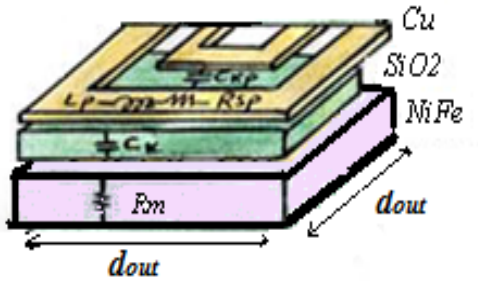


Fig 4: Geometric form of the magnetic core [12]

*Calculating of turn's number*

The primary and secondary inductances values are given by the following formulas (method Mohan) [13][14]:

(8) $$L_t = \frac{\mu . . n_t^2 . D_{moy} . C_1}{2} \left( ln\left(\frac{C_2}{\rho}\right) + \rho . C_3 + \rho^2 C_4 \right)$$

(9) $$L_b = \frac{\mu . . n_b^2 . D_{moy} . C_1}{2} \left( ln\left(\frac{C_2}{\rho}\right) + \rho . C_3 + \rho^2 C_4 \right)$$

$D_{moy}$ is the average diameter of the inductor defined from the inner diameter and outer diameter $d_{out}$ and $d_{in}$ (equation 10)[15].

(10) $$D_{moy} = \frac{d_{out} + d_{in}}{2} = 1350 \mu m$$

$\rho$ is the form factor, defined by relationship (11)

(11) $$\rho = \frac{d_{out} - d_{in}}{d_{out} + d_{in}} = 0.33$$

$C_1$, $C_2$, $C_3$, $C_4$ are the constants of Mohan given by table2.

Table 2: the constants of mohan

| Geometry | $C_1$ | $C_2$ | $C_3$ | $C_4$ |
|---|---|---|---|---|
| Square | 1.27 | 2.07 | 0.18 | 0.13 |

The primary and secondary turn's numbers are calculated by using expressions 12 and 13

(12) $$n_t = \sqrt{\frac{2 L_t}{\mu . D_{moy} . C_1 \left( ln\left(\frac{C_2}{\rho}\right) + \rho . C_3 + \rho^2 C_4 \right)}}$$

(13) $$n_b = \sqrt{\frac{2L_b}{\mu.D_{moy}.C_1\left(ln\left(\frac{C_2}{\rho}\right)+\rho.C_3+\rho^2C_4\right)}}$$

After calculation, we find: $n_t = 5,\ n_b = 2$ .

*Calculating the width of the primary and secondary conductors*

To eliminate the skin effect so that the electrical current is distributed over the entire section of the conductor, one of the following conditions must be satisfied: $W \le 2\delta$ or $t \le 2\delta$ Where w and t the width and thickness of the conductor. For a frequency f = 40 MHz, $\rho_{copper}=1{,}7.10^{-8}$ *[Ω.m]* and $\mu_r=1$ *[H/m]* a skin thickness δ is obtained by used of equation 14 [16]:

(14) $$\delta = \sqrt{\frac{\rho}{\pi.\mu_0.f}} = 10.38\,\mu m$$

We impose one of two values *W* or t and compute the second. It is preferable to impose the value of the thickness t of the conductor, since the width w should be optimized to reduce the parasitic effects linked to the substrate and the core. By assigning to "t" a value that verifies ≤ 2δ , we can calculate the width by the used of equation 15.

(15) $$S = W.t$$

When a current $I$ flows in a conductor of section $S$ its current density $J_{avg}$ is given by expression16.

(16) $$I = S.J_{avg}$$

The surface current density in a conductor of rectangular section is expressed by the relations 17 and 18.

(17 ) $$\overline{j(x)} = j_0.e^{-j(\frac{x}{\delta})}.e^{-(\frac{x}{\delta})}$$

(18) $$j(x) = j_0.e^{-(\frac{x}{\delta})}$$

(19) $$j_{avg} = \frac{1}{\delta}\int_0^{\delta} j(w)\,dw = \frac{1}{\delta}\int_0^{\delta} j_0 e^{\frac{-w}{\delta}}dw = j_0\left(1-e^{-1}\right) \approx 0.63\,j_0$$

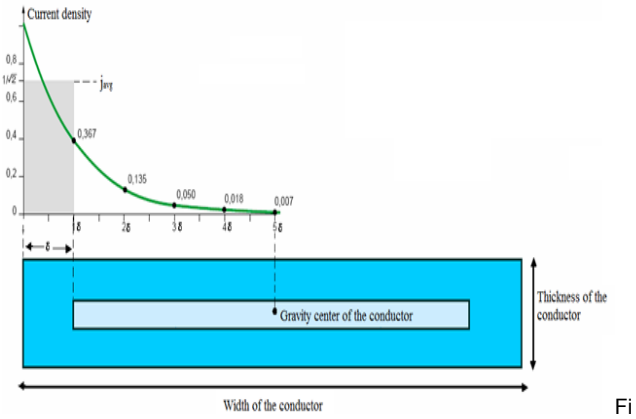


Fig 5 : Decrease of the current density inside a

In most cases, the micro-wires are in contact with a semiconductor substrate which has good heat conduction properties. This allows to pose as boundary conditions $J_o = 10^9\ A/m^2$ [15].

If we apply equations 15 to 19 to the primary and secondary windings and by considering the same surface current density in the two windings, and the same thickness value of the primary and secondary conductors t, we obtain the following results. Results are obtained by putting $t = 20.76\ \mu m.$ $W_t = 45\,\mu m$ and $W_b = 196.87\,\mu m$

*Calculation of primary and secondary inter-turn's spacing $S_t$ and $S_b$*

(20) $$S_t = (d_{out} - d_{in} - 2W_t.n_t)/2(n_t - 1)$$

(21) $$S_b = (d_{out} - d_{in} - 2W_b.n_b)/2(n_b - 1)$$

*Calculation of primary and secondary conductor length*

(22) $$l_t = 4.n_t(d_{out} - (n_t - 1).S_t - n_t.W_t) - S_t$$

(23) $$l_b = 4.n_b(d_{out} - (n_b - 1).S_b - n_b.W_b) - S_b$$

All parameters that go into the design of the micro-transformer are represented in the below summary table

table 3: values of the geometrical parameters of micro- transformer

| Geometrical parameters | Values |
|---|---|
| Outer diameter: $d_{out}$ | 1800 µm |
| Inner diameter: $d_{in}$ | 900 µm |
| Core thickness: e | 16.15 µm |
| Skin thickness: δ | 10.38 µm |
| Number of primary turns: $n_t$ | 5 |
| Number of secondary turns: $n_b$ | 2 |
| Width of the primary $W_t$ | 45 µm |
| Width of the secondary : $W_b$ | 196.87 µm |
| Thickness of the primary: $t_t$ | 20.76 µm |
| Thickness of the secondary: $t_b$ | 20.76 µm |
| Primary spacing: $S_t$ | 56.25 µm |
| Secondary spacing: $S_b$ | 56.25 µm |
| Primary total length: $l_t$ | 2.7 cm |
| Secondary total length: $l_b$ | 1.07 cm |

The obtained results are in agree with integration, because the values of the different geometric parameters are in the recommended dimensions for the integration in low power electronics.

**Modeling of Micro-Transformer**

The use of S-parameters will help to determine the values of the primary and secondary inductances, the primary and secondary series resistors and the quality factor. The calculation with the S-parameters is made from the π-electric model of the micro-transformer Figure 6 by following these steps:

*We calculate the ABCD matrices for each block*

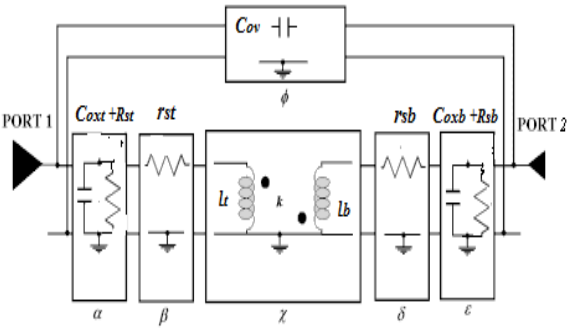


Fig 6: *ABCD* Network Model of integrated transformer [8]

(24) $$\begin{bmatrix} A & B \\ C & D \end{bmatrix}_{\alpha} = \begin{bmatrix} 1 & 0 \\ \frac{1}{j\omega C_{oxt}} + \frac{R_{st}}{1+j\omega R_{st}C_{st}} & 1 \end{bmatrix}$$

(25) $$\begin{bmatrix} A & B \\ C & D \end{bmatrix}_{\beta} = \begin{bmatrix} 1 & r_{st} \\ 0 & 1 \end{bmatrix}$$

(25) $$\begin{bmatrix} A & B \\ C & D \end{bmatrix}_{\gamma} = \begin{bmatrix} \frac{l_t}{M} & j\omega(\frac{l_t l_b}{M} - M) \\ \frac{1}{j\omega M} & \frac{l_b}{M} \end{bmatrix}$$

(26) $$\begin{bmatrix} A & B \\ C & D \end{bmatrix}_{\delta} = \begin{bmatrix} 1 & r_{sb} \\ 0 & 1 \end{bmatrix}$$

(27) $$\begin{bmatrix} A & B \\ C & D \end{bmatrix}_{\varepsilon} = \begin{bmatrix} 1 & 0 \\ \dfrac{1}{\dfrac{1}{j\omega C_{oxb}} + \dfrac{R_{sb}}{1 + j\omega R_{sb} C_{sb}}} & 1 \end{bmatrix}$$

(28) $$\begin{bmatrix} A & B \\ C & D \end{bmatrix}_{\phi} = \begin{bmatrix} 1 & \dfrac{1}{j\omega C_{ov}} \\ 0 & 1 \end{bmatrix}$$

(29) $$M = k.\sqrt{l_t l_b}$$

*We combine the cascade blocks* $\alpha, \beta, \chi, \delta, \varepsilon$

(30) $$\begin{bmatrix} A & B \\ C & D \end{bmatrix}_{1} = \begin{bmatrix} A & B \\ C & D \end{bmatrix}_{\alpha} . \begin{bmatrix} A & B \\ C & D \end{bmatrix}_{\beta} . \begin{bmatrix} A & B \\ C & D \end{bmatrix}_{\delta} . \begin{bmatrix} A & B \\ C & D \end{bmatrix}_{\chi} . \begin{bmatrix} A & B \\ C & D \end{bmatrix}_{\tau} . \begin{bmatrix} A & B \\ C & D \end{bmatrix}_{\varphi}$$

*We combine the large intermediate I block with the block F in parallel. The final matrix ABCD of the entire micro transformer F is given below:*

(31) $$\begin{bmatrix} A & B \\ C & D \end{bmatrix}_{F} = \frac{1}{B_I + B_\varphi} . \begin{bmatrix} A_I.B_\varphi + A_\varphi.B_I & B_I.B_\varphi \\ (C_I + C_\varphi).(B_\varphi + B_I) + (D_I - D_\varphi).(A_\varphi - A_I) & D_\varphi.B_I + D_I.B_\varphi \end{bmatrix}$$

*We transform parameters A, B, C, D as follows* [18]:

(32) $$S_{11} = \frac{A + \dfrac{B}{Z_0} - C_F.Z_0 - D}{A + \dfrac{B}{Z_0} + C.Z_0 + D}$$

(33) $$S_{12} = \frac{2.(A.D - (B.C))}{A + \dfrac{B}{Z_0} + C.Z_0 + D}$$

(34) $$S_{21} = \frac{2}{A + \dfrac{B}{Z_0} + C.Z_0 + D}$$

(35) $$S_{22} = \frac{-A + \dfrac{B}{Z_0} - C.Z_0 + D}{A + \dfrac{B}{Z_0} + C.Z_0 + D}$$

$S_{11}$, $S_{12}$, $S_{21}$, $S_{22}$ are the S parameters. $Z_0$ = 50 Ω is the characteristic impedance of the line. In addition, because of reciprocity, we will have $AD - BC = 1$. Therefore, $S_{12} = S_{21}$. From the low-frequency S-parameters, the Z-parameters at each frequency point are determined. This can be shown as follows :

(36) $$Z_{11} = Z_0 \frac{(1 + S_{11}).(1 - S_{22}) + S_{21}.S_{12}}{(1 - S_{11}).(1 - S_{22}) - S_{12}.S_{21}}$$

(37) $$Z_{21} = Z_{12} = Z_0 \frac{2.S_{12}}{(1 - S_{11}).(1 - S_{22}) - S_{12}.S_{21}}$$

(38) $$Z_{22} = Z_0 \frac{(1 + S_{11}).(1 - S_{22}) + S_{21}.S_{12}}{(1 - S_{11}).(1 - S_{22}) - S_{12}.S_{21}}$$

From these equations, we find the variables that make up the model Pi shown in Figure 6 and the inductances of the primary $L_t$ and secondary $L_b$. These inductances are taken from the imaginary part of the impedances, are expressed by expressions (39-40) [18][19].

(39) $$L_t = \frac{Im(Z_{11})}{\omega}$$

(40) $$L_b = \frac{Im(Z_{22})}{\omega}$$

And series resistors of the integrated inductors $r_{st}$ (primary) and $r_{sb}$ (secondary) are extracted from the real part of the impedances and are expressed by expressions (41-42) [20][21].

(41) $$r_{st} = Re(Z_{11})$$

(42) $$r_{sb} = Re(Z_{22})$$

The expressions of quality factors extracted from the real and imaginary part of the impedances are given by expressions (43-44) [22][23].

(43) $$Q_t = \frac{Im(Z_{11})}{Re(Z_{11})}$$

(44) $$Q_b = \frac{Im(Z_{22})}{Re(Z_{22})}$$

From the three-dimensional section of a micro-transformer, is deduced the equivalent electric circuit Figure 7.

The transformer as seen in figure 7 is an assembly of micro-ribbons or propagation lines isolated by an insulating material (silicon dioxide), superimposed between two silicon (substrate) layers, surmounted Two layers of magnetic material (ferrite) and two layers of insulating material (silicon dioxide). Therefore, it can be modeled from the basic elements of the circuits: inductors, resistors and capacitors.

The transformer model figure 8 is similar to model spiral inductor spiral. Indeed, the transformer is simply a pair of spiral inductor magnetically coupled. This model includes the series inductances of the primary and secondary coils ($L_t$ , $L_b$), the series resistances of second primary coil ($r_{st}$,$r_{sb}$), the coupling capacitances between the turns ($C_{ov1,2}$), the capacities between the secondary and primary coils and the substrate ($C_{oxt}$, $C_{oxb}$), the substrate capacity of primary and secondary coils ($C_{st}$,$C_{sb}$) [ 24].

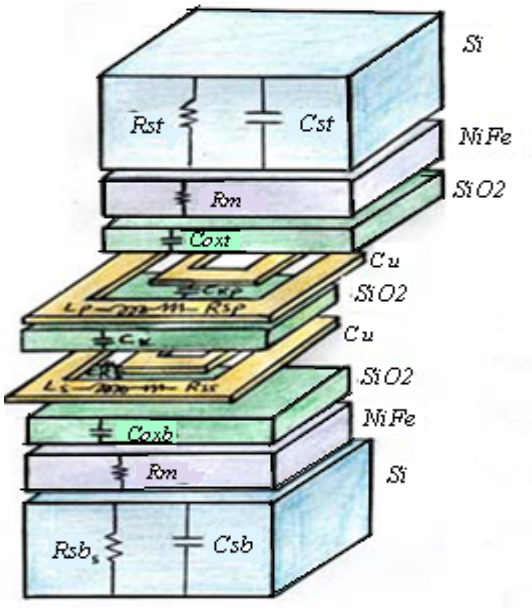


Fig 7: The three-dimensional section of a micro-transformer

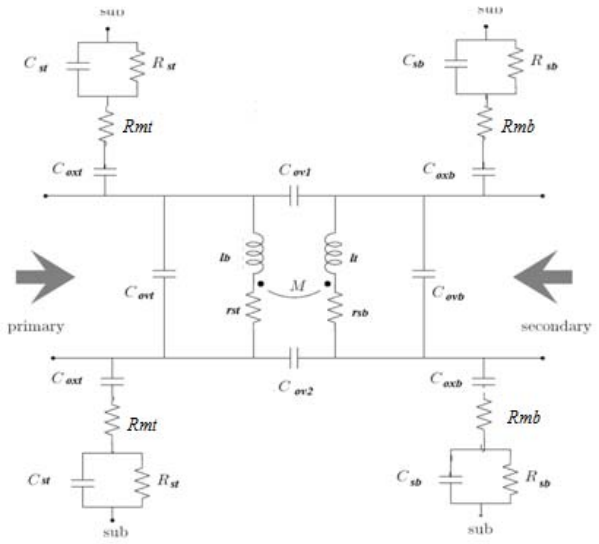


Fig.8 : Model of the equivalent electrical circuit of micro-transformer[14]

***Calculation of the electrical parameters***

We present now the analytical expressions of the electrical circuit's different elements [8]:

The series resistance: $r_{st}$ ,$r_{sb}$ . lt and lb are respectively, the primary and the secondary lengths:

(45) $$r_{st} = \frac{\rho.l_t}{W_t.\delta.(1-e^{\frac{t}{\delta}})}$$

(46) $$r_{sb} = \frac{\rho.l_b}{W_b.\delta.(1-e^{\frac{t}{\delta}})}$$

The oxide capacities: $C_{oxt}$, $C_{oxb}$

(47) $$c_{oxt} = \frac{.\varepsilon_{ox}}{2.t_{ox,t}}.W_t.l_t$$

(48) $$c_{oxb} = \frac{.\varepsilon_{ox}}{2.t_{ox,b}}.W_b.l_b$$

The coupling capacitance between the turns $C_{ovt}$ ,$C_{ovb}$ $C_{ov1,2}$:

(49) $$c_{ovt} = \frac{\varepsilon_{ox}}{2.S_t}(t_t.l_t)$$

(50) $$c_{ovb} = \frac{\varepsilon_{ox}}{2.S_b}(t_b.l_b).$$

(51) $$c_{ov1} = \frac{\varepsilon_{ox}.W_t.l_t}{t_{ox}}$$

(52) $$c_{ov2} = \frac{\varepsilon_{ox}.W_b.l_b}{t_{ox}}$$

The substrate capacity of primary and secondary coils: $C_{st}$,$C_{sb}$ :

(53) $$c_{st} = \frac{\varepsilon_{si}.l_t.W_t}{2.e_{si}}$$

(54) $$c_{sb} = \frac{\varepsilon_{si}.l_b.W_b}{2.e_{si}}$$

The substrate resistance of the primary and secondary coils: $R_{st}$, $R_{sb}$

(55) $$R_{st} = \frac{2.\rho_{si}.e_{si}}{l_t.W_t}$$

(56) $$R_{sb} = \frac{2.\rho_{si}.e_{si}}{l_b.W_b}$$

(57) $$R_{mt} = \rho_{Nife}\frac{e_{Nife}}{l_t.W_t}$$

(58) $$R_{mb} = \rho_{Nife}\frac{e_{Nife}}{l_b.W_b}$$

***Results of electrical parameter's calculation***

The table 4 summarizes the different calculated electrical parameters.

Table 4: values of micro-transformer's electrical parameters

| Electrical parameters | Values |
|---|---|
| primary inductance $L_t$ | 52nH |
| secondary inductance $L_b$ | 8.3 nH |
| Primary serial resistance $r_{st}$ | 1.11Ω |
| Secondary serial resistance $r_{sb}$ | 0.10 Ω |
| Primary oxide capacitance $C_{oxt}$ | 2.96 pF |
| Secondary oxide capacitance $C_{oxb}$ | 5.08 pF |
| Primary résistance of substrate $R_{st}$ | 2.99 KΩ |
| Secondary résistance of substrate $R_{sb}$ | 1.74 KΩ |
| Primary capacitance of du substrat $C_{st}$ | 0.64pF |
| Secondary capacitance of substrate $C_{sb}$ | 1.10 pF |
| Capacitance inter-spacing of primary $C_{ovt}$ | 0.16 pF |
| Capacitance inter-spacing of secondary $C_{ovb}$ | 0.064 pF |
| Coupling capacitance between the primary and secondary coils $C_{ov1}$ | 5.45 pF |
| Coupling capacitance between the secondary and primary coils $C_{ov2}$ | 10.05pF |
| Primary magnetic resistance *Rmt* | 5.22μΩ |
| Secondary magnetic resistance *Rmb* | 3.04μΩ |

***Results interpretation***

The objective of geometrical dimensioning of a transformer is to reduce its volume, as well as energy losses. To reach this objective, the technological parameters must verify the following conditions:

The capacities $C_{oxt}$, $C_{oxb}$, $C_{st}$, $C_{sb}$, should be as low as possible to avoid any infiltration of current into the core and into the substrate.

The capacitances $C_{ovt}$ and $C_{ovb}$ must be very low in order to avoid short circuits between the turns of the primary and secondary coils.

The capacitances $C_{ov1}$ and $C_{ov2}$ must also be very low in order to avoid short circuits between the primary coil and the secondary coil.

The resistances $R_{mb}$, $R_{mt}$, $R_{sb}$ and $R_{st}$, must be as high as possible in order to prevent the passage of currents induced by capacitive effect.

On the other hand, the resistances $\boldsymbol{r_{sb}}$ and $\boldsymbol{r_{st}}$ must be very low in order to reduce the losses by joule effects and to facilitate the circulation of the current in the primary and secondary.

We conclude that, the obtained results are in agreement with the desired objectives.

***Influence of frequency on the inductances of the primary and secondary***

Figure 9 shows the influence of the frequency on the inductances of the primary $L_t$ and secondary $L_b$. These inductances are extracted from the imaginary part of the impedances and are expressed by the expressions (39) and (40) [18][19].

The figure above shows two distinct zones specific to the operation of the integrated inductors (primary and secondary). At the operating frequency (40MHz), we recognize the inductive behavior. Beyond the resonance frequency (80MHz), it is the capacitive behavior [25].

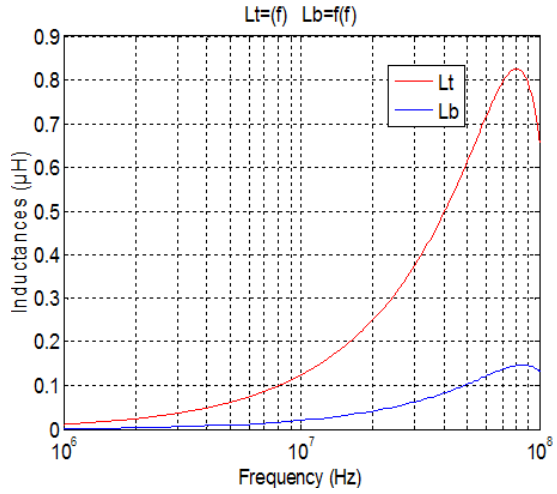


Fig.9 : Influence of the operating frequency on the value of $L_t$ and $L_b$ inductors

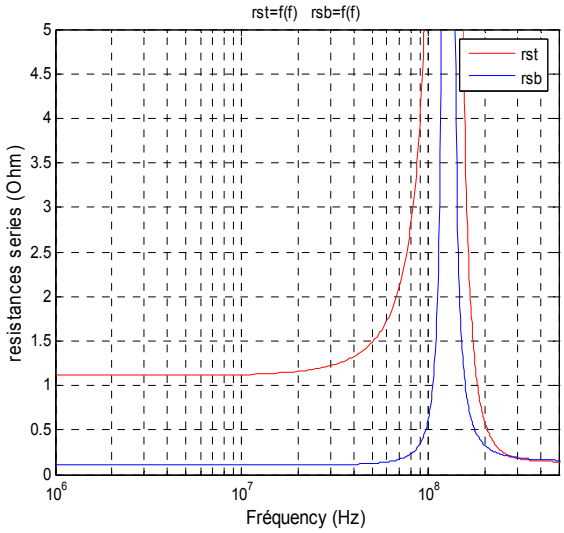


Fig.10 influence of primary and secondary series resistance versus frequency

***Influence of frequency on the series resistances of the primary and secondary***

Figure 10 shows the influence of the frequency on the series resistors $r_{st}$ of primary and $r_{sb}$ of secondary. These resistances are extracted from the real part of the impedances and are expressed by expressions (41) and (42) [20][21].

The resistances $r_{st}$ and $r_{sb}$ have very low values at the operating frequency ( 40 MHz), so the losses by Joule effects are very low. At resonance, the primary and secondary series resistances result in a peak.

***Influence of frequency on the quality factor of primary and secondary inductances***

Figure 11 shows the influence of the frequency on the quality factors of inductors primary and secondary. The expressions of quality factors extracted from the real and imaginary impedances are given by the expressions (43) and (44) [22][23].

We note in figure.11 that the quality factor increases with the frequency until reaching a maximum value corresponding to the operating frequency 40 MHz. It reaches 10 for the primary winding and 20 for the secondary winding at 40 MHz.. The quality factor decreases to zero at an operating point corresponding to the resonance frequency.

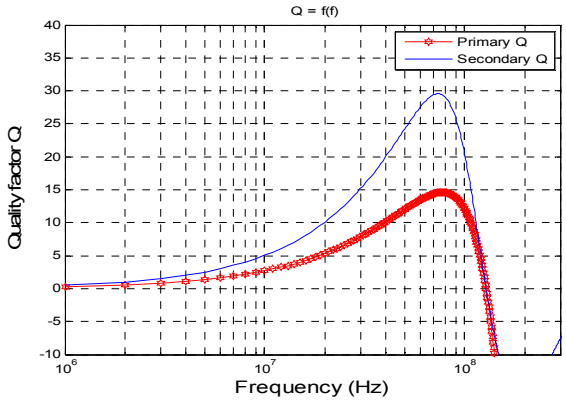


Fig.11 Quality factor of primary and secondary versus frequency

**Simulation of The Equivalent Electrical Circuit**

Simulations have conducted to determine the influence of losses on the micro converter. The PSIM 6.0 software has been selected to simulate the operation of the converter.

we need to calculate the following three electrical parameters of the micro converter [11].

Load resistance of the Fly-back converter

(59) $$R_s = \frac{V_s}{i_s} = 2.66\Omega$$

Capacity of the fly-back converter, for a voltage undulation equal to 0.01V, the capacitor C is equal to:

(60) $$C_s = \frac{\alpha^2 m V_e}{(1-\alpha)\Delta V_s R_s f} = 1.87\text{x}10^{-6}\ \text{F}$$

Magnetizing inductance

(61) $$L_m = n_t^2 \frac{\mu_{Nife} d_{out}^{\ 2}}{2e} \approx 2.5\text{mH}$$

***Ideal transformer***

The transformer that we will place in the converter is lossless (ideal). The electrical circuit of the assembly is given in Figure12.The simulation of voltages and currents are done using the software PCIM6.0

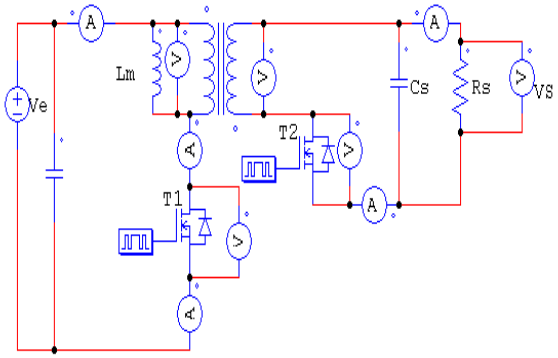


Fig. 12: Equivalent electrical circuit of the converter with an ideal transformer

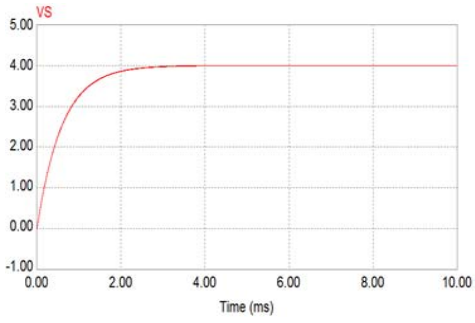


Fig.13: Output voltage of the converter with an ideal Transformer

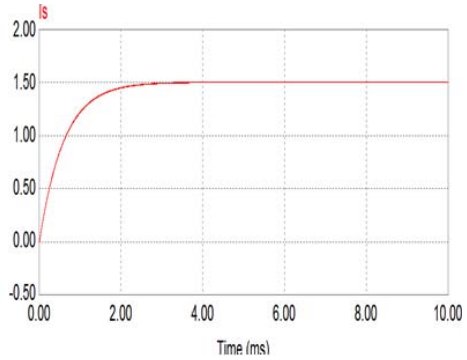


Fig.14: Output current of the converter with an ideal Transformer

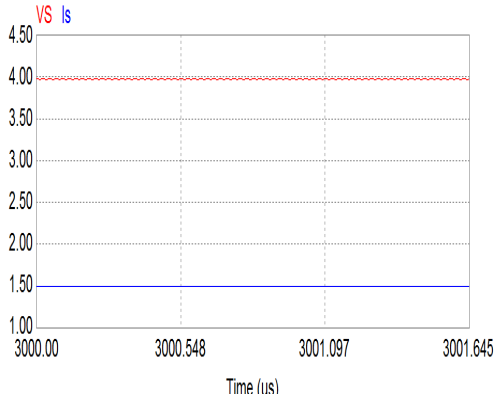


Fig.15: Waveforms of the output voltage and the output current of the converter containing an ideal transformer

Table 5: maximum measured values, output voltage and output current ideal transformer

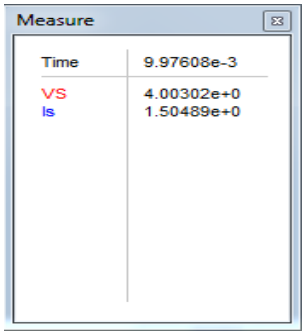


We note that the voltage and output current levels Figure 13 and Figure 14 are consistent with those contained in the specification, the micro-transformer being ideal. Also Figure 15 shows the Zoom of waveforms without ideal values.

***Real transformer***

The microc-onverter comprises a real transformer Figure 16. So it includes additional elements such as primary leakage inductance $L_{ft}$ and secondary leakage inductance $L_{fb}$, the primary winding resistance $r_{st}$ and resistance of the secondary winding leakages $r_{sb}$ [26][27].

$$L_{ft} = n_t^2 . \frac{\mu_{cu} . W_t . t_t}{2 . l_t} \quad (62)$$

$$L_{fb} = n_b^2 . \frac{\mu_{cu} . W_b . t_b}{2 . l_b} \quad (63)$$

In the case of the real micro transformer, the voltage and output current levels Figure. 17 are consistent with those contained in the specification. We observe, in this case, a slight discrepancy between these results and those of the specifications. Figure 18 shows the zoom of waveforms without slight offset to specification.

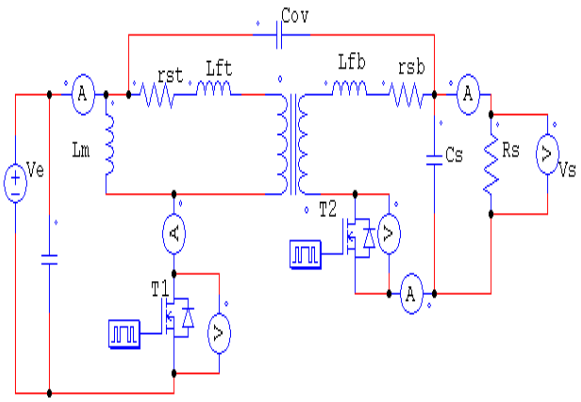


Fig 16: Equivalent electrical circuit of the converter with a real transformer

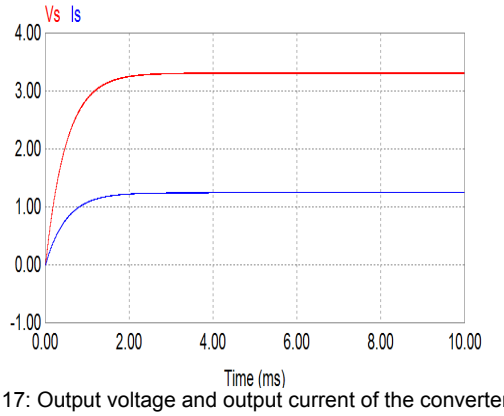


Fig.17: Output voltage and output current of the converter with a real transformer

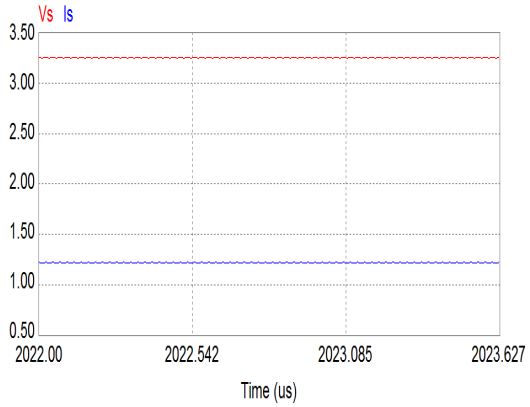


Fig.18: Waveforms of the output voltage and the output current of the converter containing a real transformer

Table 6: maximum measured values, output voltage andoutput current real transformer

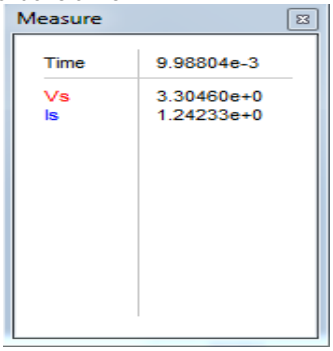

***Integrated transformer***

After modeling and simulation of ideal and real transformer, we now simulate the equivalent circuit of the converter containing the micro transformer.

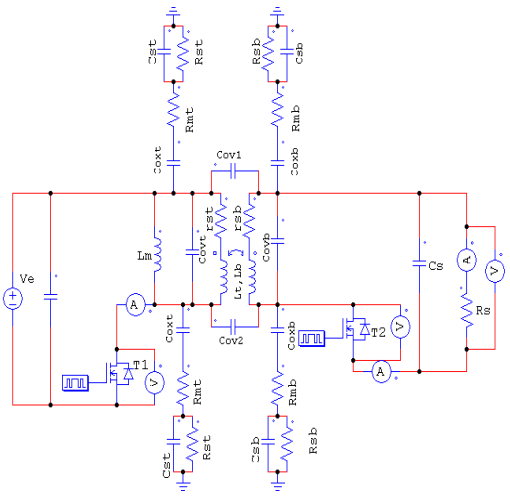


Fig. 19: Equivalent electrical circuit of the micro converter containing the integrated transformer

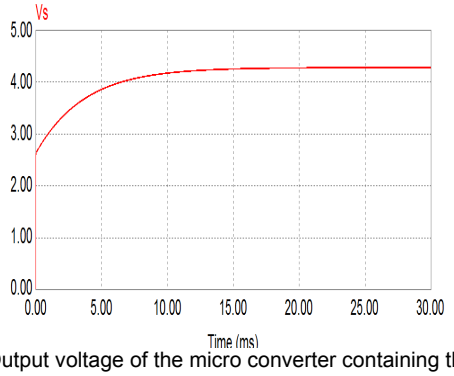


Fig.20: Output voltage of the micro converter containing the integrated transformer

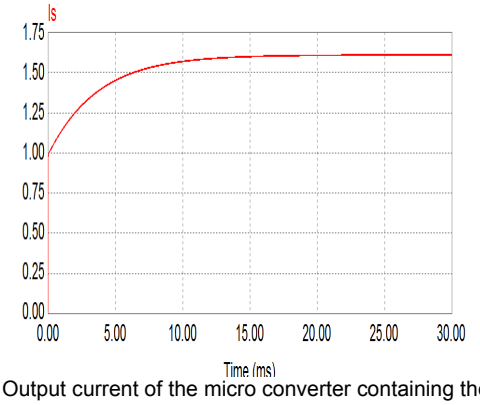


Fig. 21: Output current of the micro converter containing the integrated transformer

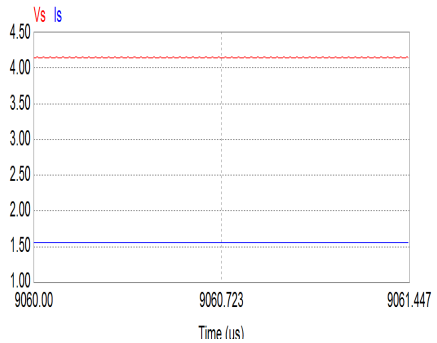


Fig.22: Waveforms of the output voltage and the output current of the micro converter containing an integrated transformer

table 7: maximum measured values, output voltage and output current integrated transformer

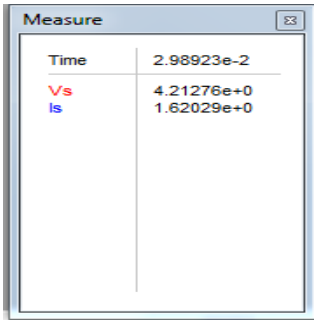


***Results interpretation***

For the ideal transformer, the results of the simulation in figures 13, 14 and 15 are excellent: the output current and the output voltage are continuous and in accordance with the specifications (Vs= 4V and Is =1.5A). In the case of the real transformer (Figures 17 and 18), the current and the output voltage are continuous, but their values are somewhat low compared to the values of the specifications (Vs= 3.30Vand Is =I.24A). Whereas for integrated transformers ( Figures 20, 21 and 22), the results are encouraging because we have a continuous output voltage and a continuous output current and their values are very close to those of the specifications (Vs= 4.2V and Is = 1.6A).

Therefore, we conclude that the geometrical dimensioning of the transformer gave good results.

***The Flyback Converter Efficiency***

The fly back converter efficiency is the ratio between of output power and input power[28].

$$\eta = \frac{p_s - p_j - p_f}{p_s} \quad P_s = V_s.I_s \text{ is output power,}$$

,

$P_j = R_{seq}.I_s^2$ is Joule losses , $P_f = \frac{V_e^2}{R_{sub}}$ is iron losses

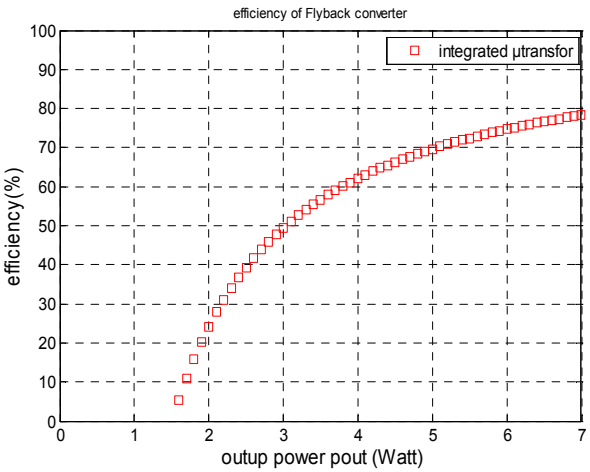


Fig.23: Fly back converter efficiency as a function of output power

The curves in Figure 23 show the evolution of the output as a function of the output power in the case of integrated micro-transformer. We note that the yield at point 6 W corresponding to 1.5A and 4 V (specifications) is 76%. This value is explained by the different losses and drops of voltages at the level of our micro-converter.

## Simulation of Different Effects On The Micro Transformer

In this section, we present the distribution of magnetic field lines in the micro-coils of the micro transformer.

Using the FEMLAB 3.1 software, we observe in figure 25 an overflow of the magnetic field lines in all directions. These lines occupy all the space and are stopped only by the simulation boundaries of a coil in the air. This distribution can induce disturbances of the components located in the immediate vicinity of the micro transformer.

In figure 26, the coils are deposited on a magnetic core, the majority of these field lines being confined in this core. This is explained by the high permeability of ferrite. The insertion of the ferrite layers thus makes it possible to increase the number of magnetic field lines and to limit their overflow

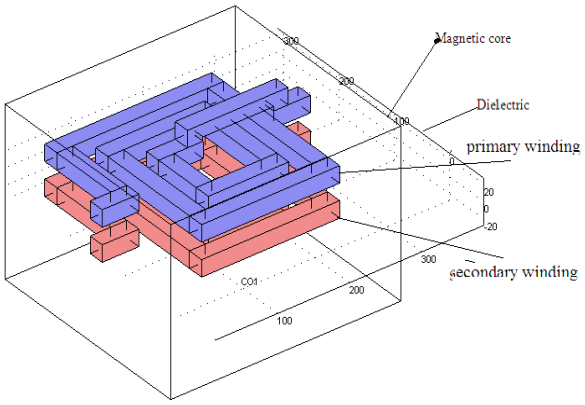


Fig.24: View 3D of the primary and secondary micro coils

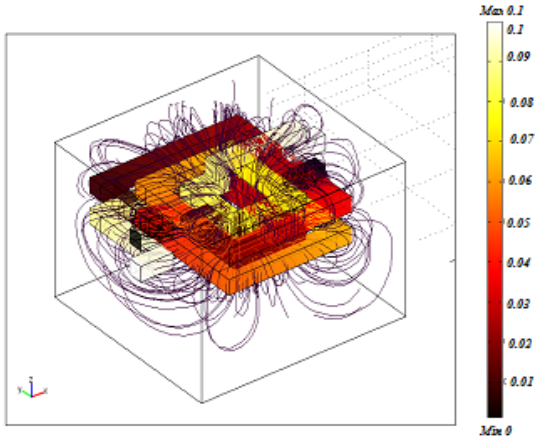


Fig.25: Magnetic field distribution in the micro-transformer without magnetic core

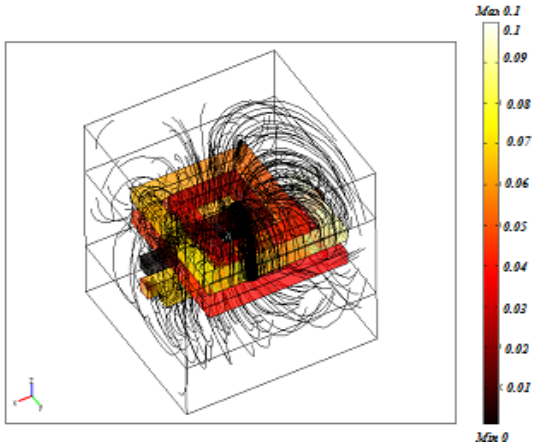


Fig.26: Magnetic field distribution in the micro-transformer with a magnetic core

## Conclusion

The aim of this study is the geometrical dimensioning of a micro-transformer and its electromagnetic modeling to integrate it into a micro-converter. This micro-transformer is intended for the field of mobile and embedded electronics requiring a conversion of energy of low power and a very high frequency range. The integrated micro-transformer is composed of several stacked layers, namely: two copper square planar coil windings, insulating layers, layers of ferrite magnetic material and a semiconductor layers.

As a starting point for our study, we chose the specifications of the fly-back type micro-converter. In the second part, according to the operating conditions of the system based on the method of Mohan, we carried out the geometrical dimensioning of the planar transformer. The geometric dimensioning is carried out in order to reduce the volume of the micro-transformer, as well as the energy losses while meeting the specifications.

In the third part, we used the geometric parameters to extract the various electrical parameters. From the calculated values of the electrical parameters, we have deduced that the parasitic effects have been very considerably reduced.

In the last step, we integrated the dimensioned micro-transformer into a micro-converter . This step allowed to test the good operation of the micro-transformer. In order to validate our results, we performed a simulation with PSIM6.0 software. So, we compared the output voltage and output current of the micro-converter in the case of three transformers: an ideal transformer, a real transformer and the integrated micro-transformer. The waveforms of the currents and voltages of the micro converter containing the integrated transformer were in accordance with those of the literature and the measured values were very close to its specifications.

The transformer composed of different materials stacked on each other, generates parasitic effects, notably at high and very high frequencies. In order to choose the transformer which gives the best results, we used the simulation software FEMLAB 3.1 to visualize the dispersion of the magnetic field lines for two different transformer models, A model with core, and the second without core.

***Abdelkader ABDELDJEBBAR[1]*, Azzedine HAMID[1], Yacine GUETTAF[2], Rabia MELATI[1]***

*[1] Laboratory of Applied Power Electronics (LEPA), University of Sciences and Technology Mohamed Boudiaf of Oran (USTO-MB), ALGERIA.*

*[2] University Center Nour Bachir of El Bayadh, ALGERIA.*

*Corresponding author e-mail: abdeldjebbar@yahoo.com*

## REFERENCES

[1] KhamisYoussouf. "Modélisation des transformateurs planaires intègres. Optics / Photonic".Université Jean Monnet-Saint-Etienne, 2014.France.

[2] Dagal Dari Yaya. "Conception, réalisation et caractérisation d'inductances planaires à couches magnétiques", Université Jean Monnet - Saint-Etienne, 2013. France.

[3] BENJAMIN VALLET "Étude et conception d'une nouvelle alimentation à découpage à transfert d'énergie mixte basée sur un composant passif LCT intégré" Université Joseph Fourier 2008

[4] Abdelhadi BESRI "Modélisation analytique et outils pour l'optimisation des transformateurs de puissance haute fréquence planars" 26 mai 2011université De Grenoble

[5] TrungHieu TRINH "Réseaux de micro convertisseurs, les premiers pas vers le circuit de puissance programmable" 09 Janvier 2013.

[6] Fred C. Lee and J. D. van Wyk "IPEM-Based Power Electronics System Integration", Journal of Electrical Engineering www.jee.ro

[7] R. Melati, A. Hamid, F. Baghdad, F. Taibi, "Simulation d'une micro bobine", Département d'Electrotechnique, Faculté de Génie Electrique, Université des sciences et de la technologie d'Oran (USTO). 4ème Conférence Internationale sur l'Electrotechnique ICEL'09, 10-11 Novembre 2009.
[8] ShwetabhVerma and Jose M. Cruz "On-chip Inductors and Transformers", December 1999.
[9] Fu Keung Wong, B. Eng, M. Phil, "High Frequency Transformer for Switching Mode Power Supplies", School of Microelectronic Engineering, Faculty of Engineering and Information Technology, Griffith University, Brisbane, Australia, March 2004
[10] V. Boyer, N. Godefroy, "Alimentation à découpage Flyback", M1-IUP GEII, Université Joseph Fourier IEEE.
[11] M. Derkaoui, A. Hamid,T. Lebey, R. Melati, " Design and Modeling of an Integrated Micro-Transformer in a Flyback Converter", Telecommunication, Computing, Elctronics and Control, Telkomnika, Scopus Vol. 11, N° 4, pp. 669~682, December 2013. ISSN: 1693-6930. journal.uad.ac.id/ HYPERLINK "Chap5.pdf"index.php Hyperlink Chap5.pdf"/Telkomnika/article/view/1785
[12] D. M. Pozar "Microwave Engineering", Second Edition. JohnWiley and Sons Inc., 1998, pp.19-20, pp. 182-250.
[13] S. Mohan, C.P.Yue, M. del Mar Hershenson, S. Wong, and T.H. Lee, "Modeling and characterization of on-chip transformers," *International Electron Devices Meeting 1998*, Technical Digest, IEEE, 1998, pp. 531-534.
[14] Sunderarajan,S.Mohan"the design modeling and optimization of on-chip inductor and transformer circuits" December 1999.
[15] C Alonso "Contribution à l'optimisation, la gestion et le traitement de l'énergie", Université PaulSabatier – Toulouse III. 2003.
[16] X.Margueron "Elaboration sans prototypage du circuit équivalent des transformateurs de type planar" ,Laboratoire d'Electrotechnique de Grenoble, Université Joseph Fourier, 23 octobre 2006.
[17] A. Duluzaux, "Pertes supplémentaires dans les conducteurs pour forte intensité par effet de peau et de proximité ", Collection Technique de Schneider Electric, Edition N° 83, pp. 4-19, Janvier 1977
[18] R. Thüringer "Characterization of Integrated Lumped Inductors and Transformers",Wien University, April 2002.
[19] AndreasWeisshaar "Analysis and Modeling of Monolithic On-Chip Transformers on Silicon", June 10, 2005.
[20] Y. K. Koutsoyannopoulos, "Systematic Analysis and Modeling of Integrated Inductors and Transformers in RF IC Design", Analog and Digital Signal Processing, vol.47, no. 8, august 2000 699.
[21] D. Kehrer"Design of Monolithic Integrated Lumped Transformers in Silicon-based Technologie sup to 20 GHz", Wien University, December 2000.
[22] XuDaoxian "Characterization and modeling of Micro-wave spiral ransformers and inductors", Peking University, China, 2005.
[23]"Stacked Inductors and Transformers in CMOS Technology",ieee journal of solid-state circuits, vol. 36, no. 4, april 2001
[24] JosepCabanillas Costa "Analysis of Integrated Transformers And its Application To Rfic Design", Barcelona, Octubre 2002.
[25] Philippe Artillan "Conception, modélisation et réalisation de composants inductifs intégrés pour alimentations de faible puissance et micro systèmes ",27 novembre 2008l'Université de Toulouse
[26] Bastien ORLANDO "Conception, Réalisation et Analyse de Micro-Inductances Intégrées avec Matériaux Ferromagnétiques Doux", Soutenue le 5 Février 2007 à Limoges
[27] J .Y.s Le Chenadec "Alimentation à découpage, Etude, dimensionnement des alimentations à découpage usuelles", Lycée Louis Armand, Strasbourg 22octobre2001 .
[28] Alberto M Pernía, Miguel J Prieto, Juan M Lopera. "High Power Density DC/DC Converter Using Thick-Film Hybrid Technology" Universidad de Oviedo. Campus de Viesques. Gijón (Asturias). Spain.